

Structural and microscopic relaxations in a colloidal glass

Flavio Augusto de Melo Marques^{*a}, Roberta Angelini^{b,c}, Emanuela Zaccarelli^{c,d}, Bela Farago^e, Beatrice Ruta^f, Giancarlo Ruocco^{a,c}, Barbara Ruzicka^{b,c}

The aging dynamics of a colloidal glass has been studied by multiangle Dynamic Light Scattering, Neutron Spin Echo, X-ray Photon Correlation Spectroscopy and Molecular Dynamics simulations. The two relaxation processes, microscopic (fast) and structural (slow), have been investigated in an unprecedentedly wide range of time and length scales covering both ergodic and nonergodic regimes. The microscopic relaxation time remains diffusive at all length scales across the glass transition scaling with wavevector Q as Q^{-2} . The length-scale dependence of structural relaxation time changes from diffusive, characterized by a Q^{-2} -dependence in the early stages of aging, to Q^{-1} -dependence in the full aging regime which marks a discontinuous hopping dynamics. Both regimes are associated with a stretched behaviour of the correlation functions. We expect these findings to provide a general description of both relaxations across the glass transition.

1 Introduction

The dynamical behaviour of glass-forming systems has long been the subject of intense research¹. One important feature of disordered systems is that the dynamics of density fluctuations is characterized by a two-step decay, which implies the presence of two main relaxation processes²: a microscopic or fast relaxation, associated to the interactions between a particle and the cage of its nearest neighbors followed by a structural or slow relaxation process, related to the structural rearrangements of the particles. These two distinct processes have been observed in simple monatomic liquids³, hydrogen bonded liquids^{4,5}, structural glasses^{6–8}, colloids^{9–11} and DNA nanostars¹². Furthermore Mode Coupling Theory (MCT)¹³ has predicted the evolution of the two relaxations when a system goes from the liquid to the arrested state: this may happen e.g. by changing temperature, packing fraction or waiting time (aging). However, even if the supercooled liquid

phase above T_g in glass forming materials has been widely investigated with both DLS^{7,14} and neutron scattering techniques^{15–19}, it is still not clear how the two relaxation processes behave at the liquid-glass transition. While in a liquid the dynamics is known to be diffusive, a change in particle dynamics should occur, as found in numerical simulations^{20,21}, from diffusive to activated in the glass. The signature of this change at different length scales can be revealed by investigating the wavevector Q dependence of the relaxation times. Several numerical studies on different systems such as water²², ortho-terphenyl²³ and hard spheres²⁴ reported a subquadratic dependence of the structural relaxation time approaching the glass state. A recent theoretical work based on activated MCT has rationalised these findings providing a microscopic explanation for the change of dynamics across the glass transition²⁵. So far, there has been no clear experimental proof of this scenario due to technical difficulties. Moreover, a full description encompassing both relaxation processes and their behaviour at different length scales is missing. This is the aim of the present work where the aging investigation of a colloidal system makes possible a detailed study across the glass transition, in particular increasing waiting time in this system plays the same role as decreasing temperature in glass forming systems²⁶.

In this paper we study the aging dynamics of a colloidal glass, monitoring the waiting time t_w and wavenumber Q dependence of both fast $\tau_1(Q)$ and slow $\tau_2(Q)$ relaxation times through a combination of multiangle Dynamic Light Scattering (DLS), Neutron Spin Echo (NSE), X-Ray Photon Correlation Spectroscopy (XPCS) and Molecular Dynamics (MD) simulations. In this way we access an unprecedentedly wide range of time and length scales and we find a different behaviour for the two relaxations across the glass transition. While the microscopic one remains unperturbed, indicating an unchanged, diffusive single particle dynamics at short times, the structural relaxation shows a clear change. Indeed, τ_2 going from the liquid to the arrested state undergoes a transition from a Q^{-2} to a Q^{-1} behaviour. Pioneering works by Bonn and coworkers^{11,27} in aqueous Laponite dispersions reported a Q^{-2} dependence for both microscopic and structural relaxation times in the ergodic DLS regime. Later on works on different systems e.g. colloids^{28,29}, clays^{30–33}, metallic glasses³⁴, polymers^{35–37}, supercooled liquids³⁸ reported a Q^{-1} dependence of the structural relaxation time associated to

^a Center for Life Nano Science, IIT@Sapienza, Istituto Italiano di Tecnologia, Viale Regina Elena 291, 00161 Roma, Italy. Tel: +39 06 4991 3505; E-mail: flavio.marques@iit.it

^b IPCF-CNR, I-00185 Roma, Italy.

^c Dipartimento di Fisica, Sapienza Università di Roma, I-00185, Italy.

^d ISC-CNR, I-00185 Roma, Italy.

^e Institute Laue-Langevin, BP 156, 38042 Grenoble, France.

^f European Synchrotron Radiation Facility, B.P. 220 F-38043 Grenoble, Cedex France.

an anomalous compressed exponential relaxation of the correlation functions attributed to a hyperdiffusive dynamics³⁹. Differently, in the present work the relaxation curves at long times are always described by a stretched exponential, which allow us to interpret the crossover from a Q^{-2} to a Q^{-1} across the glass transition as a signature of a change from diffusive dynamics to discontinuous hopping of caged particles, as predicted in²⁵.

2 Materials and Methods

We used a widely studied colloidal clay^{40–46}, Laponite RD dispersions, prepared using the same protocol described in Ref.⁴⁶. All measurements have been performed using D_2O (EURISO-TOP) of purity $\geq 99.9\%$ as a solvent. As recently shown the H/D isotopic substitution, required to gain contrast in neutron scattering measurements, does not qualitatively affect the aging behaviour of Laponite⁴⁷. The waiting time origin ($t_w = 0$) is the time at which the dispersion is filtered (and sealed) directly in glass tubes with diameter of 10 mm for DLS and of 2 mm for XPCS and in quartz cells with dimensions of 30 mm \times 40 mm \times 4 mm for NSE measurements. All experiments were performed at the same molar concentration of a $C_w = 3.0\%$ sample in salt free water. At this weight concentration the system forms a Wigner glass^{27,48} due to repulsive electrostatic interactions. This is a glass occurring in a dilute system which shares the main features of denser glasses, including a two-step decay^{49–51}.

DLS measurements were performed with a multi-angle setup in the time range between 10^{-6} s and 1 s. A solid state laser with wavelength of 642 nm and power of 100 mW and single mode collecting fibers at five different scattering angles are used. Time autocorrelation functions are therefore simultaneously acquired at wavenumbers $Q = 6.2 \times 10^{-4}$, 1.1×10^{-3} , 1.5×10^{-3} , 1.8×10^{-3} and $2.1 \times 10^{-3} \text{ \AA}^{-1}$ by calculating the intensity autocorrelation function as $g_2(Q, t) = \frac{\langle I(Q, t_0)I(Q, t_0+t) \rangle}{\langle I(Q, t_0) \rangle^2}$ where $\langle \dots \rangle$ denotes the temporal average over t_0 . DLS are used only when the system is ergodic in the early aging, also referred as cage forming, regime characterized by a structural relaxation time with a waiting time exponential dependence $\tau_2(t_w) \propto e^{t_w}$ ⁴².

XPCS measurements were performed at the ID10 beamline at the European Synchrotron Radiation Facility (ESRF, Grenoble, France) in a Q -range between 3.1×10^{-3} and $2.2 \times 10^{-2} \text{ \AA}^{-1}$ including the peak of the static structure factor occurring at $Q_{peak} \sim 1.6 \times 10^{-2} \text{ \AA}^{-1}$ as in H_2O solvent⁴⁸. Using an incident partially coherent X-ray beam with energy fixed at 8 keV a series of scattering images were recorded by a charged coupled device (CCD) and the ensemble averaged intensity autocorrelation function $g_2(Q, t)$ was calculated by using a standard multi tau algorithm after having ensemble aver-

aged over the detector pixels mapping onto a single Q value⁵². XPCS can thus be used when the system is non ergodic in the full aging regime characterized by a waiting time power law dependence of the structural relaxation time $\tau_2(t_w) \propto t_w^\alpha$ with $\alpha \sim 1$ ⁴².

NSE measurements were performed at the spectrometer IN15 of the Institute Laue-Langevin (ILL, Grenoble, France) at larger wavevectors ($1.3 \times 10^{-2} < Q < 1.3 \times 10^{-1} \text{ \AA}^{-1}$) and at shorter relaxation times (up to 2×10^{-7} s) with respect to DLS and XPCS. We used wavelength of 10, 16 and 22.8 \AA yielding time ranges (0.35 - 50) ns, (1.4 - 206) ns and (4.1 - 598) ns respectively. While DLS and XPCS measure the normalized intensity correlation function $g_2(Q, t) = 1 + b[g_1(Q, t)]^2$ (Siegert relation), respectively through temporal averages (ergodic regime) and ensemble averages (non ergodic regime), NSE directly accesses the intermediate scattering function $g_1(Q, t)^2$.

We complement the experimental measurements with MD simulations for a simple model of low-density glass-former, i.e. a 50 – 50 non-crystallising binary mixture of $N = 1000$ Yukawa particles of equal screening length ξ and different repulsion strength^{50*}. The system was found⁵⁰ to undergo a Wigner glass transition upon decreasing temperature T . To mimic the experimental situation, we performed a quench inside the glassy region at fixed number density $\rho = 0.002984$. The system was equilibrated at high $T = 1.0 \times 10^{-3}$ and then instantaneously quenched to $T = 1.6 \times 10^{-5}$, below the glass transition occurring at $T_g \sim 1.7 \times 10^{-5}$. The waiting time origin was the time of the quench. Self intermediate scattering functions $F^s(Q, t)$ have been calculated for different wave vectors as a function of waiting time, averaging over 20 independent quenches to improve statistics.

3 Results

Figure 1(a) shows the normalized intensity correlation functions measured by DLS at initial waiting time ($t_w = 9$ min) for different Q -values (symbols) and the corresponding fits (full lines) obtained through a typical double exponential decay:

$$g_2(q, t) - 1 = b \left[a e^{-\left(\frac{t}{\tau_1}\right)^\gamma} + (1 - a) e^{-\left(\frac{t}{\tau_2}\right)^\beta} \right]^2 \quad (1)$$

where the parameters a and $(1 - a)$ are the amplitudes of the two relaxation modes, b is the coherence factor, τ_1 is the fast relaxation time connected to the microscopic motion of particles, τ_2 is the slow relaxation time related to the structural rearrangement, γ (here $\gamma=1$ ^{11,53}) and β measure the distribution widths of the two relaxations.

*Lengths and times are measured in units of ξ and $\xi/(m\varepsilon)^{1/2}$ respectively, where m is the mass of the particles and ε is the unit of energy. Temperature is measured in units of ε (i.e. $k_B=1$ where k_B is the Boltzmann constant).

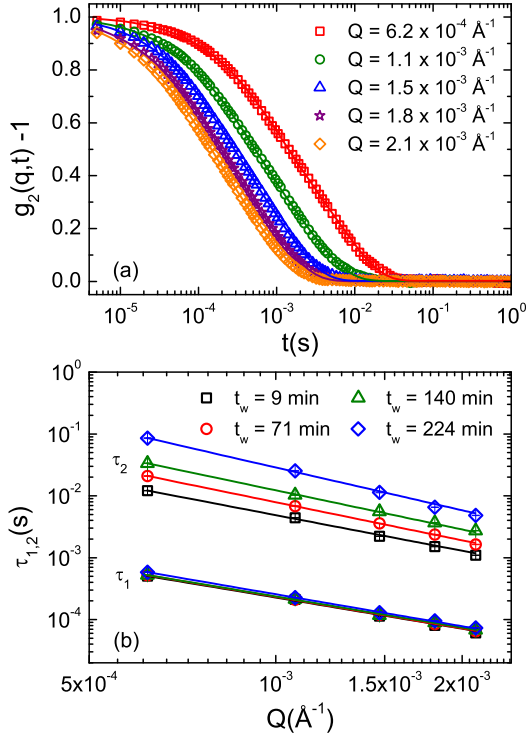


Fig. 1 (a) Normalized intensity correlation functions measured through DLS for different Q -values at $t_w = 9$ min. Solid lines are the fits obtained through Eq. 1 with $\gamma=1$. (b) Q -dependence of the fast τ_1 and slow τ_2 relaxation times at different waiting times. Solid lines are power law fits of the data as $\sim Q^{-n}$ where $n=1.70 \pm 0.06$ for τ_1 and $n=2.02 \pm 0.19$ for τ_2 .

The Q -dependence of the fast and slow relaxation times is reported in Fig. 1(b) at different waiting times. While τ_1 shows a moderate waiting time dependence, τ_2 increases significantly with t_w . Both times are well described by power law fits $\sim Q^{-n}$ with $n \sim 2$ (solid lines in Fig. 1(b)). Hence both microscopic and structural relaxation times display an almost quadratic wave vector dependence in the DLS (early aging) regime, which is the signature of diffusive dynamics for both relaxations at these early waiting times. These findings are in agreement with the works on Laponite water suspensions by the group of Bonn et al.^{11,27} and of Munch et al.^{32,33}. Fig. 2(a) shows the dynamic structure factors measured by NSE at different wavevectors (symbols) together with single stretched exponential fits (full lines). The corresponding fast relaxation times are shown in Fig. 2(b). We find that τ_1 scales as $\sim Q^{-2}$ during the whole experiment. As reported in the inset of Fig. 2(b) the estimate of τ_1 obtained from the NSE fits is in good agreement with that obtained by DLS, taking into account the large difference in Q between these techniques. Since the studied sample experiences a sol to Wigner glass transition at $t_w \approx 600$ min, NSE results ensure that the

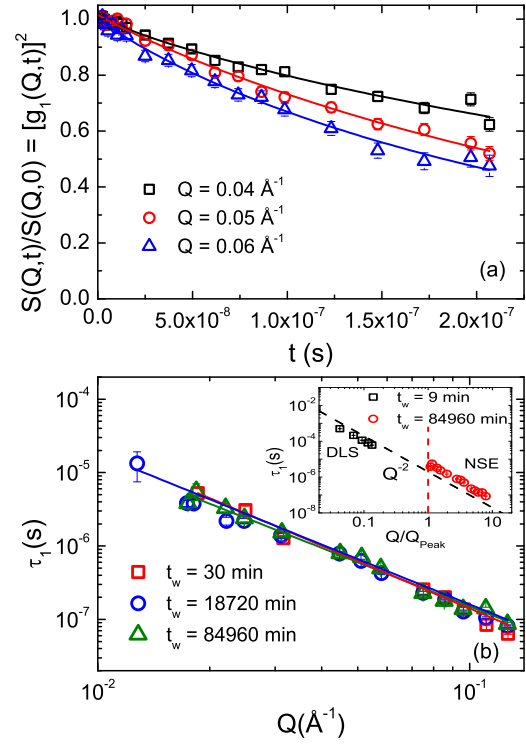


Fig. 2 (a) Dynamic structure factor obtained from NSE measurements for different Q -values at $t_w = 30$ min. Solid lines are stretched exponential fits with $\beta \sim 1$. (b) Q -dependence of the fast relaxation time at different waiting times. Solid lines are power law fits of the data as $\sim Q^{-n}$ where $n=1.97 \pm 0.24$. Inset: comparison between fast relaxation times measured through DLS ($t_w=9$ min) and NSE ($t_w=84960$ min) as a function of Q/Q_{peak} . The dashed line indicates the Q^{-2} behaviour. The red vertical line indicates the position of the structure factor peak.

microscopic relaxation time remarkably scales as Q^{-2} both in the early aging and full aging regimes indicating that the short-time dynamics remains diffusive for all the investigated dynamical range even in the arrested state.

In Fig. 3(a) normalized intensity correlation functions probed by XPCS in the full aging regime are shown at different Q -values (symbols). At these long waiting times the fast relaxation time τ_1 is out of the XPCS detection window. Hence only the slow relaxation time τ_2 can be measured and only the second term of Eq. 1 is used to fit the data (full lines in Fig. 3(a)). We notice that in our case DLS measurements allow to probe relaxation times up to $\sim 10^{-1}$ s (higher limit in Fig. 1 (b)), reached for the sample in the ergodic region at waiting time $t_w=224$ min, while XPCS measurements permit to access relaxation times above $\sim 10^2$ s (lower limit in Fig 3b) achieved for the sample in the non ergodic region at waiting times $t_w=743$ min. Figure 3(b) shows the Q -dependence of τ_2 at different waiting times (symbols) and

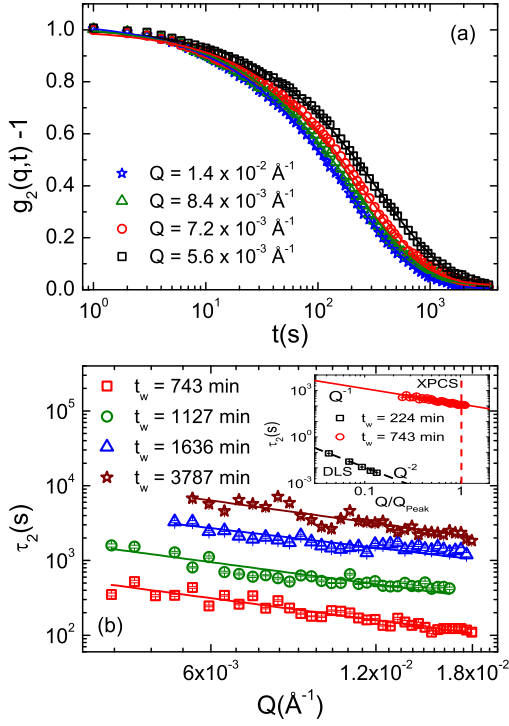


Fig. 3 (a) Normalized intensity correlation functions measured through XPCS for different Q -values at $t_w = 1127$ min. Solid lines are the fits obtained through the stretched exponential decay. (b) Q -dependence of the slow relaxation time at different waiting times. Solid lines are power law fits of the data as $\sim Q^{-n}$ where $n = 0.95 \pm 0.12$. Inset: comparison between slow relaxation times measured through DLS ($t_w = 9$ min) and XPCS ($t_w = 743$ min) as a function of Q/Q_{peak} . The dashed and full lines indicate respectively the Q^{-2} and Q^{-1} behaviours. The red vertical line indicates the position of the structure factor peak.

the associated power law fits (full lines) as $\sim Q^{-n}$. In this regime we find $n \simeq 1$ ruling out diffusive dynamics. Therefore a crossover from the DLS early aging regime characterized by $\tau_2(Q) \propto Q^{-2}$, $\tau_2(t_w) \propto e^{t_w}$ to the XPCS full aging regime characterized by $\tau_2(Q) \propto Q^{-1}$, $\tau_2(t_w) \propto t_w^\alpha$ with $\alpha \sim 1$ is observed. In both cases the intensity correlation functions are described by stretched exponentials at variance with the $\beta > 1$ behaviour found in previous works^{30–33} and in rejuvenated samples⁵⁴, as fully discussed in Ref.⁵⁴.

The combination of three complementary experimental techniques has allowed us to show that the fast relaxation mode remains diffusive both in ergodic and non-ergodic conditions at all waiting times. On the other hand, we observe that the structural relaxation time is characterized by two distinct Q behaviours in the two different t_w regimes. It remains to elu-

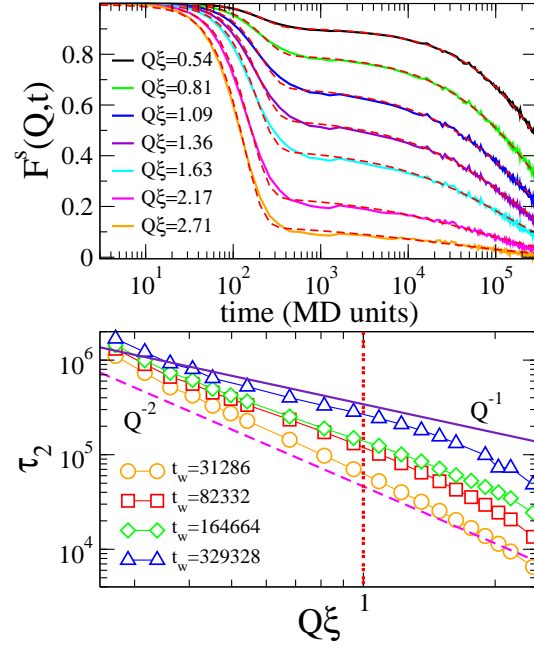


Fig. 4 (a) Self intermediate scattering functions (full lines) from MD simulations following a quench to $T = 1.6 \times 10^{-5}$ at fixed waiting time $t_w = 329328$ MD units and different wave vectors, as reported in the labels. Dashed lines are the fitting curves obtained using the expression within the square brackets of Eq. 1 with $\gamma=2$. (b) Q -dependence of the slow relaxation time τ_2 extracted from the fits for selected values of t_w . The dashed and full lines indicate respectively the Q^{-2} and Q^{-1} behaviours. The red vertical line indicates the position of the structure factor peak.

cidate what happens in between the DLS and XPCS regimes, i.e. whether the change is discontinuous or not. Bhattacharyya et al.²⁵ have predicted a gradual change of the dynamics. To address this point we turn to MD simulations.

In Fig. 4(a) we report the MD self intermediate scattering functions (full lines) at fixed waiting time after a quench in the glassy state for several wavevectors. The microscopic dynamics is Newtonian, thereby the data are fitted by the double exponential decay within the square brackets of Eq. 1 fixing $\gamma=2$ and the corresponding τ_1 is not relevant to describe the experimental (Brownian) fast relaxation. We discuss only wavevectors small enough that the second exponential in Eq. 1 is stretched ($\beta < 1$), excluding large Q values where the dynamics becomes again ballistic due to the underlying microscopic dynamics⁵⁵. In the early aging regime, the correlators do not display the typical two-step decay, similarly to what observed in out-of-equilibrium simulations of other glass formers⁵⁶. We thus focus on the regime occurring at larger waiting times, i.e. $t_w \gtrsim 20000$, where full aging starts and the double exponential describes the correlators, as shown by the fits in Fig. 4(a) (dashed lines). The corresponding τ_2 is reported as

a function of Q in Fig. 4(b) for different values of the waiting time. We find that τ_2 initially displays a Q^{-2} dependence at low and intermediate wave-vectors, in agreement with the DLS data of Fig. 1. Upon increasing t_w , while at low Q (approaching the hydrodynamic regime) τ_2 still tends to recover a diffusive behaviour (Q^{-2}), at intermediate Q encompassing the main structure factor peak (see vertical line in Fig. 4b) a clear power-law dependence Q^{-n} with the exponent lowering and approaching unity at large t_w , is observed. At even larger t_w the system becomes non-ergodic on the timescale of our simulations. Thus, in the full aging regime we observe a strongly non-diffusive dependence of τ_2 , approaching a Q^{-1} behaviour, in full agreement with the XPCS data in the same Q -window. Interestingly, n decreases continuously with increasing t_w in agreement with theoretical predictions²⁵.

4 Conclusions

In this work we have investigated the Q -dependence of both microscopic and structural relaxation times during the early aging and full aging regimes of a colloidal glass through multi-angle DLS, NSE and XPCS techniques, covering a wide range of wavevectors and times. The experimental results have been complemented by MD simulations. We found that the microscopic relaxation time, τ_1 , characteristic of the short-time diffusion of a particle in the suspending medium, scales as Q^{-2} during both early aging and full aging regimes, depicting a diffusive nature of particles motion. On the contrary the slow relaxation time, τ_2 , associated to the structural rearrangement of the system, shows a transition from a Q^{-2} diffusive behaviour in the liquid (or early aging) regime to a Q^{-1} activated dynamics in the glass (or full aging) regime associated with a stretched behaviour of the correlation functions, in full agreement with recent theoretical predictions²⁵. The reported experimental evidence is not specific to the studied system, but appears to have an intrinsic generality, occurring also in numerical studies on different glass-formers²²⁻²⁴. Therefore our study of both relaxations in an aging colloidal system may provide a general description of the complex dynamics at fast and slow timescales of any glass-former.

5 Acknowledgments

We acknowledge ILL and ESRF for beamtime and Orsolya Czakkel for providing assistance during the XPCS measurements. RA and EZ acknowledge support from MIUR-PRIN. EZ acknowledges support from MIUR-FIRB ANISOFT (RBFR125H0M).

References

1 P. G. Debenedetti and F. H. Stillinger, *Nature* **410**, 259 (2001).

2 U. Balucani and M. Zoppi, *Dynamics of the Liquid State* (Clarendon Press - Oxford, 1994).

3 T. Scopigno, U. Balucani, G. Ruocco, and F. Sette, *Phys. Rev. Lett.* **85**, 4076 (2000).

4 R. Angelini, P. Giura, G. Monaco, G. Ruocco, F. Sette, and R. Verbeni, *Phys. Rev. Lett.* **88**, 255503 (2002).

5 G. Monaco, A. Cunsolo, G. Ruocco, and F. Sette, *Phys. Rev. E* **60**, 5505 (1999).

6 F. Mezei, W. Knaak, and B. Farago, *Phys. Rev. Lett.* **58**, 571 (1987).

7 D. L. Sidebottom, R. Bergman, L. Borjesson, and L. M. Torell, *Phys. Rev. Lett.* **71**, 2260 (1993).

8 M. Zuriaga, L. C. Pardo, P. Lunkenheimer, J. L. Tamarit, N. Veglio, M. Barrio, F. J. Bermejo, and A. Loidl, *Phys. Rev. Lett.* **103**, 075701 (2009).

9 S. Z. Ren and C. M. Sorensen, *Phys. Rev. Lett.* **70**, 1727 (1993).

10 W. van Meegen and S. M. Underwood, *Physical Review Letters* **70**, 2766 (1993).

11 B. Abou, D. Bonn, and J. Meunier, *Phys. Rev. E* **64**, 021510 (2001).

12 S. Biffi, R. Cerbino, F. Bomboi, E. Paraboschia, R. Asselta, F. Sciortino, and T. Bellini, *PNAS* **24**, 15633 (2013).

13 W. Götze, *Complex Dynamics of Glass-Forming Liquids: A Mode-Coupling Theory* (Oxford Science Publications - Oxford, 2008).

14 D. L. Sidebottom, B. V. Rodenburg, and J. R. Changstrom, *Phys. Rev. B* **75**, 132201 (2007).

15 F. Mezei and W. Knaak, *Phys. Scripta* **T19**, 363 (1987).

16 A. Tolle, *Rep. Prog. Phys.* **64**, 1473 (2001).

17 A. Arbe, J. Colmenero, F. Alvarez, M. Monkenbusch, D. Richter, B. Farago, and B. Frick, *Phys. Rev. Lett.* **89**, 245701 (2002).

18 B. Farago, A. Arbe, J. Colmenero, R. Faust, U. Buchenau, and D. Richter, *Phys. Rev. E* **65**, 051803 (2002).

19 J. Colmenero, F. Alvarez, Y. Khairy, and A. Arbe, *J. Chem. Phys.* **139**, 044906 (2013).

20 L. Angelani, R. DiLeonardo, G. Ruocco, A. Scala, and F. Sciortino, *Phys. Rev. Lett.* **85**, 5356 (2000).

21 K. Broderix, K. K. Bhattacharya, A. Cavagna, A. Zippelius, and I. Giardinina, *Phys. Rev. Lett.* **85**, 5360 (2000).

22 F. Sciortino, P. Gallo, P. Tartaglia, and S. H. Chen, *Phys. Rev. E* **54**, 6331 (1996).

23 A. Rinaldi, F. Sciortino, and P. Tartaglia, *Phys. Rev. E* **63**, 061210 (2001).

24 E. J. Saltzman and K. S. Schweizer, *Phys. Rev. E* **74**, 061501 (2006).

25 S. M. Bhattacharyya, B. Bagchi, and P. G. Wolynes, *J. Chem. Phys.* **132**, 104503 (2010).

26 F. Sciortino, C. D. Michele, S. Corezzi, J. Russo, E. Zaccarelli, and P. Tartaglia, *Soft Matter* **5**, 2571 (2009).

27 D. Bonn, H. Tanaka, G. Wegdam, H. Kellay, and J. Meunier, *Europhys. Lett.* **45**, 52 (1999).

28 L. Cipelletti, S. Manley, R. C. Ball, and D. A. Weitz, *Phys. Rev. Lett.* **84**, 2275 (2000).

29 A. Duri, T. Autenrieth, L.-M. Stadler, O. Leupold, Y. Chushkin, G. Grubel, and C. Gutt, *Phys. Rev. Lett.* **102**, 145701 (2009).

30 M. Bellour, A. Knaebel, J. L. Harden, F. Lequeux, and J. P. Munch, *Phys. Rev. E* **67**, 031405 (2003).

31 R. Bandyopadhyay, D. Liang, H. Yardimci, D. A. Sessoms, M. A. Borthwick, S. G. J. Mochrie, J. L. Harden, and R. L. Leheny, *Phys. Rev. Lett.* **93**, 228302 (2004).

32 S. Kaloun, R. Skouri, M. Skouri, J. P. Munch, and F. Schosseler, *Phys. Rev. E* **72**, 011403 (2005).

33 F. Schosseler, S. Kaloun, M. Skouri, and J. P. Munch, *Phys. Rev. E* **73**, 021401 (2006).

34 B. Ruta, Y. Chushkin, G. Monaco, L. Cipelletti, E. Pineda, P. Bruna, V. M. Giordano, and M. Gonzalez-Silveira, *Phys. Rev. Lett.* **109**, 165701 (2012).

-
- 35 P. Falus, M. A. Borthwick, S. Narayanan, A. R. Sandy, and S. G. J. Mochrie, *Phys. Rev. Lett.* **97**, 066102 (2006).
 - 36 S. Narayanan, D. R. Lee, A. Hagman, X. Li, and J. Wang, *Phys. Rev. Lett.* **98**, 185506 (2007).
 - 37 H. Guo, G. Bourret, M. K. Corbierre, S. Rucareanu, R. B. Lennox, K. Laaziri, L. Piche, M. Sutton, J. L. Harden, and R. L. Leheny, *Phys. Rev. Lett.* **102**, 075702 (2009).
 - 38 C. Caronna, Y. Chushkin, A. Madsen, and A. Cupane, *Phys. Rev. Lett.* **100**, 055702 (2008).
 - 39 J.-P. Bouchaud and E. Pitard, *Eur. Phys. J. E* **6**, 231 (2001).
 - 40 A. Mourchid, E. Lecolier, H. Van Damme, and P. Levitz, *Langmuir* **14**, 4718 (1998).
 - 41 P. Mongondry, J. F. Tassin, and T. Nicolai, *J. Colloid Interface Sci.* **283**, 397 (2005).
 - 42 H. Tanaka, S. Jabbari-Farouji, J. Meunier, and D. Bonn, *Phys. Rev. E* **71**, 021402 (2005).
 - 43 S. Jabbari-Farouji, G. H. Wegdam, and D. Bonn, *Phys. Rev. Lett.* **99**, 065701 (2007).
 - 44 H. Z. Cummins, *J. Non Cryst. Sol.* **353**, 3892 (2007).
 - 45 A. Shahin and Y. M. Joshi, *Langmuir* **26**, 4219 (2010).
 - 46 B. Ruzicka and E. Zaccarelli, *Soft Matter* **7**, 1268 (2011).
 - 47 V. Tudisca, M. Ricci, R. Angelini, and B. Ruzicka, *RSC Advances* **2**, 11111 (2012).
 - 48 B. Ruzicka, L. Zulian, E. Zaccarelli, R. Angelini, M. Sztucki, A. Moussaïd, and G. Ruocco, *Phys. Rev. Lett.* **104**, 085701 (2010).
 - 49 C. Beck, W. Härtl, and R. Hempelmann, *J. Chem. Phys.* **111**, 8209 (1999).
 - 50 E. Zaccarelli, S. Andreev, F. Sciortino, and D. R. Reichman, *Phys. Rev. Lett.* **100**, 195701 (2008).
 - 51 H. Kang, T. R. Kirkpatrick, and D. Thirumalai, *Phys. Rev. E* **88**, 042308 (2013).
 - 52 A. Madsen, R. Leheny, H. Guo, M. Sprung, and O. Czakkel, *New J. of Phys.* **12**, 055001 (2010).
 - 53 B. Ruzicka, L. Zulian, and G. Ruocco, *Phys. Rev. Lett.* **93**, 258301 (2004).
 - 54 R. Angelini, L. Zulian, A. Fluerasu, A. Madsen, G. Ruocco, and B. Ruzicka, *Soft Matter* **9**, 10955 (2013).
 - 55 S. Saw, N. L. Ellegaard, W. Kob, and S. Sastry, *Physical Review Letters* **103**, 248305 (2009).
 - 56 D. El Masri, L. Berthier, and L. Cipelletti, *Phys. Rev. E* **82**, 031503 (2010).